Investigation of Magnetic Shielding in Xenon Difluoride Using Solid-State NMR Spectroscopy and Relativistic Density Functional Theory

Michelle A. M. Forgeron, Roderick E. Wasylishen,* and Glenn H. Penner†

Department of Chemistry, Gunning/Lemieux Chemistry Centre, University of Alberta, Edmonton, Alberta, Canada T6G 2G2

Received: November 26, 2003; In Final Form: March 2, 2004

The xenon and fluorine magnetic shielding tensors, σ, of XeF_2 are characterized using solid-state ^{129}Xe and ^{19}F NMR spectroscopy and nonrelativistic and spin−orbit relativistic zeroth-order regular approximation density functional theory (ZORA DFT). Analysis of ^{129}Xe and ^{19}F NMR spectra acquired with magic-angle spinning at several spinning rates indicates that the Xe and F magnetic shielding tensors are axially symmetric, as dictated by the crystal symmetry. The isotropic ^{129}Xe chemical shift is -1603 ± 5 ppm with respect to $OXeF_4$ (neat liquid, 24 °C) and the Xe magnetic shielding anisotropy, Ω, is 4245 ± 20 ppm, the first anisotropy measured directly for a xenon compound. The parallel component of the experimentally determined xenon chemical shift tensor, $\delta_{\parallel} = -4433$ ppm differs from δ(Xe(free atom)) by ~1000 ppm, providing the first experimental demonstration that relativistic effects play an important role in the nuclear magnetic shielding for xenon. Both the sign and magnitude of the isotropic indirect $^{129}Xe,^{19}F$ nuclear spin−spin coupling constant are determined, -5560 ± 50 Hz. Analysis of the ^{19}F NMR spectra yield $\Omega(F) = 150 \pm 20$ ppm. The ZORA DFT method has been employed to calculate σ(Xe) and σ(F) for isolated XeF_2 and XeF_4 molecules, as well as σ(Kr) and σ(F) for an isolated KrF_2 molecule, at the relativistic and nonrelativistic levels of theory. Spin−orbit relativistic DFT results for Ω(Xe) are in very good agreement with those determined experimentally and highlight the importance of relativistic effects.

1. Introduction

Reports of noble gas-containing molecules are rare; however, compounds involving krypton, xenon, radon, and most recently, argon have been reported.[1−7] The diversity of molecular systems containing noble gas atoms is limited primarily because the formation of stable bonds is generally confined to highly electronegative elements such as fluorine and oxygen. One of the first xenon-containing molecules that has attracted interest from both an experimental and a theoretical point of view is xenon difluoride, XeF_2, the simplest xenon-containing neutral molecule. Since the discovery of XeF_2 in 1962, the structure and bonding, as well as the thermodynamic and spectroscopic properties of this molecule have been the subject of theoretical[8−16] and experimental scrutiny.[17−27] The linear geometry of this centrosymmetric molecule was deduced from vibrational[17] spectra and confirmed by X-ray[18] and neutron diffraction[19] studies. More accurate bond lengths, determined from rotational Raman[20] and high-resolution infrared[21] spectra have subsequently been reported.

Numerous ^{129}Xe and ^{19}F nuclear magnetic resonance (NMR) studies of XeF_2 have been undertaken both in solution and in the solid state. The earliest work, carried out by Hindermann and Falconer,[22] involved the use of solid-state ^{19}F NMR spectroscopy to measure the rigid-lattice second moment of XeF_2 at three applied magnetic field strengths, 0.7, 1.4, and 2.35 T, to determine the anisotropy of the ^{19}F magnetic shielding tensor, Ω. The value obtained, $|\Omega(F)| = 105 \pm 10$ ppm, has been quoted numerous times in the literature and has been used to estimate Ω(Xe) indirectly (vide infra). However, given the minimal data and the relatively low applied magnetic fields available for ^{19}F NMR in 1969, the reported error in Ω(F), ±10 ppm, seems modest.

Jokisaari et al. investigated the secondary isotope effect of ^{m}Xe on the ^{19}F magnetic shielding of XeF_2 in acetonitrile-d_3.[23] Xenon difluoride is an excellent candidate for this type of study given that xenon has nine stable isotopes: ^{124}Xe (0.10%), ^{126}Xe (0.09%), ^{128}Xe (1.91%), ^{129}Xe (26.4%), ^{130}Xe (4.1%), ^{131}Xe (21.2%), ^{132}Xe (26.9%), ^{134}Xe (10.4%), and ^{136}Xe (8.9%).[28] A linear relationship was found between the one-bond secondary isotope effect on the ^{19}F magnetic shielding and the relative mass factor for the xenon isotopes.

The ^{129}Xe and ^{19}F spin−lattice relaxation times, T_1, of XeF_2 in acetonitrile-d_3 have also been studied as a function of temperature and applied magnetic field strength.[24] These data indicate that for both ^{129}Xe and ^{19}F, the nuclear magnetic shielding anisotropy and spin-rotation mechanisms are the dominant T_1 mechanisms, whereas the dipole−dipole mechanism is estimated to be much less than 1%. The ^{129}Xe and ^{19}F T_1 data were further used to investigate the magnetic shielding anisotropy in XeF_2, allowing for the first indirect measurement of Ω(Xe). Two approaches were used, resulting in very different values for Ω(Xe), 2416 and 4722 ppm, and Ω(F), 105[22] and 205 ppm (vide infra). Hence, the correct values of Ω(Xe) and Ω(F) remain an unsettled issue in the literature.

The majority of previous experimental and theoretical[29−31] ^{129}Xe NMR studies focuses on Xe(g) confined to the cavities and channels of porous materials; several excellent reviews on ^{129}Xe NMR are available.[32−38] In the present study, solid-state ^{129}Xe and ^{19}F NMR spectroscopy, as well as nonrelativistic and relativistic spin−orbit zeroth-order regular approximation density functional theory (ZORA DFT) calculations, are employed

* Corresponding author. Tel: (780)492-4336. Fax: (780)492-8231. E-mail: Roderick.Wasylishen@ualberta.ca.

† On sabbatical leave from the Department of Chemistry, University of Guelph, Guelph, Ontario, Canada N1G 2W1.

10.1021/jp031279j CCC: $27.50
Published on Web 05/01/2004

to directly determine the xenon and fluorine magnetic shielding tensors of XeF_2. We report both the magnitude and sign of $^1J(^{129}Xe,^{19}F)_{iso}$ for solid XeF_2 and compare this with previous results determined from solution ^{129}Xe NMR studies of XeF_2 in various solvents,[23,39] as well as with recent ZORA DFT calculations.[15,16] Additional relativistic and nonrelativistic shielding calculations on XeF_4 and KrF_2 are presented and compared with our results for XeF_2.

2. Background Theory

Nuclear Magnetic Shielding. Nuclear magnetic shielding, σ, arises from small magnetic fields created by the circulation of electrons about a nucleus in an external applied magnetic field, $\mathbf{B}_0$. These induced magnetic fields change the NMR resonance condition. The shielding experienced by a nucleus in a molecule depends on the orientation of the molecule with respect to $\mathbf{B}_0$ and may be described by a second-rank tensor with up to nine unique components. For a linear molecule, such as XeF_2, only two principal components, $\sigma_{||}$ and $\sigma_\perp$, are required to characterize the xenon or fluorine shielding, and their shielding tensors are said to be axially symmetric. Here $\sigma_{||}$ and $\sigma_\perp$ represent the magnetic shielding when the C_∞ symmetry axis is parallel and perpendicular to $\mathbf{B}_0$, respectively. The breadth, also known as the shielding anisotropy or span, of an axially symmetric shielding tensor is defined as $\Omega = \sigma_{||} - \sigma_\perp$. The isotropic shielding, σ_{iso}, is simply equal to one-third the trace of the shielding tensor, $\sigma_{iso} = (\sigma_{||} + 2\sigma_\perp)/3$. Experimentally, one measures the isotropic chemical shift, δ_{iso}, which is the difference in the isotropic nuclear magnetic shielding of a sample with respect to that of a standard reference:

$$\delta_{iso} = \frac{\sigma(\text{ref})_{iso} - \sigma(\text{sample})_{iso}}{1 - \sigma(\text{ref})_{iso}} = \frac{\nu(\text{sample})_{iso} - \nu(\text{ref})_{iso}}{\nu(\text{ref})_{iso}} \times 10^6 \quad (1)$$

The theory of nuclear magnetic shielding was developed by Ramsey in 1953.[40] This theory remains exact in the nonrelativistic limit and, today, is recognized as being among the most influential in 20th century quantum chemistry.[41] According to Ramsey's formalism, σ may be partitioned into diamagnetic, σ^{dia}, and paramagnetic, σ^{para}, components, which depend on the ground electronic state and excited electronic states, respectively, of the molecule. For a linear molecule, the paramagnetic shielding parallel to the bond axis, $\sigma_{||}^{para}$, is exactly zero and $\sigma_{||}^{dia} \simeq \sigma(\text{free atom})$. Several experimental NMR studies demonstrate that $\sigma_{||}$ remains invariant for linear compounds and is approximately equal to σ(free atom).[42−44] The perpendicular component of the paramagnetic shielding, $\sigma_\perp^{para}$, is nonzero and difficult to determine accurately. However, Ramsey[40] and Flygare and Goodisman[45] derived a convenient connection between the nuclear magnetic shielding constant and the nuclear spin-rotation constant, c_I, based on nonrelativistic theory. For a linear molecule,

$$\sigma_\perp \approx -\left(\frac{m_p}{2m_e g_N}\right)\left(\frac{c_I}{B}\right) + \sigma^{dia}(\text{free atom}) \quad (2)$$

where m_p is the proton rest mass, m_e is the electron rest mass, g_N is the g value of the nucleus of interest, and B is the rotational constant of the molecule. Hence, one can obtain accurate values of σ^{para} indirectly through measurement of the spin-rotation constant using molecular beam or high-resolution microwave experiments.[44,46] A further important consequence of this relationship is that it allows *absolute* nuclear magnetic shielding scales to be established;[40,46] however, the shielding scales thus obtained are strictly valid in the nonrelativistic limit. The significance of relativistic effects in calculating nuclear magnetic shielding for heavy nuclei is an important issue that continues to attract a great deal of interest; here we give only a few representative references.[47−57] One result of relativistic effects on nuclear magnetic shielding is that $\sigma_{||}^{para} \neq 0$ for linear molecules; this has been recently demonstrated in a series of nonrelativistic and relativistic calculations on the hydrogen halides, HX.[57,58] Though $\sigma_{||}^{para}(X) = 0.0$ ppm for the nonrelativistic calculations, analogous relativistic calculations yield nonzero values for $\sigma_{||}^{para}(X)$ and these values become increasingly significant for the heavier halides. For example, $\sigma_{||}^{para}(F) = 3.2$ ppm for HF, whereas $\sigma_{||}^{para}(I) = 840$ ppm for HI.[58] To our knowledge, no experimental studies of linear molecules have been reported where $\sigma_{||}$ deviates significantly from σ(free atom).

3. Experimental and Computational Details

3.1. Solid-State ^{129}Xe NMR Spectroscopy. A commercial sample of XeF_2, purchased from Aldrich, was powdered and packed into a 4 mm outer diameter zirconia rotor in a nitrogen-filled glovebox and sealed with an airtight Teflon end cap. All ^{129}Xe and ^{19}F NMR experiments were carried out at room temperature using a Chemagnetics CMX Infinity spectrometer ($\mathbf{B}_0 = 4.7$ T), operating at spectrometer frequencies of 55.574 and 188.290 MHz for ^{129}Xe and ^{19}F, respectively. The magic-angle was set by maximizing the number of rotational echoes in the ^{79}Br NMR free-induction decay and spinning sidebands of the ^{79}Br NMR spectrum of KBr. One-pulse experiments were employed to acquire ^{129}Xe and ^{19}F NMR spectra. Decoupling parameters for $^{129}Xe\{^{19}F\}$ NMR spectra were optimized on a sample of Teflon using cross-polarization (CP) ($^{19}F \rightarrow {}^{13}C$) with high-power two-pulse phase modulated[59] (TPPM) ^{19}F decoupling. In the case of XeF_2, because $T_1(^{19}F)$ is very long (>100 s) compared to $T_1(^{129}Xe)$, the use of CP from $^{19}F \rightarrow {}^{129}Xe$ is not beneficial. A one-pulse experiment with TPPM ^{19}F decoupling is more efficient and, hence, was used in the present study.

Acquisition of ^{129}Xe NMR spectra employed a spectral width of 800 kHz, a $\pi/2$ pulse width of 2.0 μs, a TPPM pulse width of 4.0 μs, an acquisition time of 10.240 ms, and a pulse delay of 60 s. All ^{19}F NMR spectra were acquired using a spectral width of 200 kHz, $\pi/2$ pulse width of 2.0 μs, acquisition time of 10.240 ms, and pulse delay of 1200 s. Simulations of ^{129}Xe and ^{19}F NMR spectra were carried out using WSOLIDS[60] and/or SIMPSON.[61] To account for $^{19}F-{}^{19}F$ dipolar interactions, ^{19}F NMR spectra were also analyzed using a memory function approach, as outlined by Hirschinger and co-workers.[62]

The primary reference for ^{129}Xe NMR spectroscopy is $OXeF_4$ (neat liquid, 24 °C), which is not readily available. A secondary reference often used is Xe(g); however, given that the chemical shift of xenon gas is sensitive to pressure and temperature changes, this is not an ideal reference sample. Our ^{129}Xe NMR spectra of XeF_2 are referenced with respect to external $OXeF_4$ (neat liquid, 24 °C) at 0.0 ppm by determining the *absolute* ^{129}Xe frequency for XeF_2. First, the absolute ^1H frequencies and chemical shifts of cyclohexane ($\nu(^1H) = 200.149\,112$ MHz, $\delta(^1H)_{iso} = 1.430$ ppm) and tetramethylsilane ($\nu(^1H) = 200.148\,826$ MHz, $\delta(^1H)_{iso} = 0.0$ ppm) were determined. Next, the absolute ^1H frequency of TMS and ^{129}Xe frequency of neat, liquid $OXeF_4$ at 24 °C ($\Xi = 27.810\,186$ MHz)[63] were used to calculate the absolute ^{129}Xe frequency for $OXeF_4$ on our spectrometer ($\nu(^{129}Xe) = 55.661\,759$ MHz). This information, along with the absolute ^{129}Xe frequency of XeF_2 and eq 1, was used to determine the chemical shift of solid XeF_2. We have

taken δ(Xe(free atom)) = −5460 ppm;[37] ^{129}Xe NMR measurements of Xe (g) on our spectrometer indicate that $\delta_{iso} = -5388$ ppm when referenced with respect to Ξ for $OXeF_4$ (neat liquid, 24 °C).[63] Our ^{19}F NMR spectra are referenced with respect to the primary ^{19}F NMR chemical shift reference, CCl_3F (neat liquid), Ξ = 94.094 011 MHz.[63] The absolute ^{19}F frequency of CCl_3F (neat liquid) on our spectrometer was calculated, 188.328 058 MHz, and used to determine the ^{19}F chemical shift of solid XeF_2.

3.2. Quantum Chemical Calculations. DFT calculations of Xe, Kr, and F magnetic shielding tensors were performed using the NMR module[64] of the Amsterdam Density Functional program.[65,66] The Vosko−Wilk−Nusair (VWN) local density approximation[67] with the Becke[68]−Perdew[69] generalized gradient approximation (GGA) were used for the exchange-correlation functional. Both relativistic and nonrelativistic calculations were performed. Relativistic calculations included scalar and spin−orbit corrections and were carried out using the ZORA formalism.[70−73] The triple-ζ doubly polarized, TZ2P, Slater-type ZORA basis sets, available with the ADF program, were employed for xenon, krypton, and fluorine. Our calculations were carried out using either an IBM RS/6000 workstation or a Linux-based cluster with dual AMD 1800+ Athlon processor nodes.

DFT calculations were performed on isolated XeF_2, XeF_4, and KrF_2 molecules at their equilibrium bond lengths, r_e(Xe,F) = 1.9791 Å,[20] r_e(Xe,F) = 1.928 970 Å,[74] and r_e(Kr,F) = 1.876 93 Å,[75] respectively, determined from Raman[20] and high-resolution infrared[74,75] spectroscopy. As well, the effect of bond length variation on the Xe, Kr, and F magnetic shielding tensors of XeF_2 and KrF_2 was investigated by systematically varying r_e(Xe,F) and r_e(Kr,F) by ±0.02 in 0.01 Å increments. The shielding of the free atom values for Kr and Xe were also determined using both nonrelativistic and spin−orbit relativistic ZORA DFT.

Noteworthy is that Vaara and Pyykkö[76] recently proposed an absolute shielding scale for xenon including relativistic effects and very large basis sets and found that σ(Xe(free atom)) = 6938 ± 21 ppm. An absolute magnetic shielding scale has also been established for fluorine, where $\sigma(CFCl_3)$ = 189.9 ppm at 303 K.[77]

4. Results and Discussion

4.1. ^{129}Xe NMR Spectroscopy. Shown in Figure 1 are experimental and calculated ^{129}Xe NMR spectra of an MAS sample of XeF_2 at two different spinning frequencies. The half-height line width, $\Delta\nu_{1/2}$, of the individual spinning sidebands is 300 ± 50 Hz. The isotropic ^{129}Xe chemical shift varied slightly with spinning frequency, which is expected given the sensitivity of ^{129}Xe chemical shifts to temperature.[23] The observed isotropic chemical shift of XeF_2, $\delta_{iso} = -1603 \pm 5$ ppm, is characteristic of Xe(II) compounds.[35] Qualitatively, the extent of shielding of the xenon nucleus appears to depend on the formal oxidation state of xenon and generally follows the trend: Xe(0) > Xe(II) > Xe(IV) > Xe(VI). Xenon gas is the most shielded, $\delta_{iso} \approx -5460$ ppm,[37] and XeO_2F^+ is the least shielded xenon species, $\delta_{iso} \approx +704$ ppm, known to date.[78] Several reports in the literature state that the xenon of XeO_6^{4-} is the least shielded xenon; however, the previously reported chemical shift for XeO_6^{4-}, +2077 ppm,[79] is erroneous and the correct value is −748 ppm.[35]

The X-ray crystal structure of XeF_2 has been determined[19] and a model of the unit cell is shown in Figure 2. In crystalline XeF_2, the molecules are aligned parallel in a body-centered array (space group $I4/m$) and the unit cell contains a total of nine

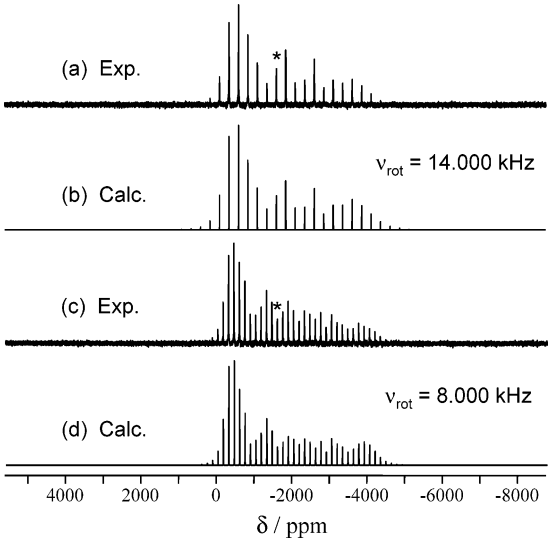

Figure 1. Experimental (a), (c) and calculated (b), (d) ^{129}Xe{^{19}F} NMR spectra of an MAS sample of XeF_2 acquired with high-power TPPM ^{19}F decoupling. The half-height line width of the spinning sidebands, $\Delta\nu_{1/2}$, is 300 ± 50 Hz. $\delta(^{129}Xe)_{iso}$ is indicated by an asterisk in (a) and (c).

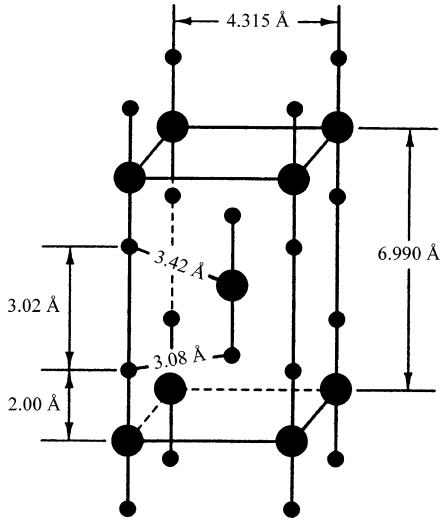

Figure 2. Unit cell of solid XeF_2 from ref 19: large spheres = xenon, small spheres = fluorine.

XeF_2 molecules. On the basis of symmetry arguments, the xenon and fluorine nuclear magnetic shielding tensors of solid XeF_2 must be axially symmetric, as evidenced by the line shape of the ^{129}Xe NMR spectra (Figure 1). Of particular note is the enormous span, $\Omega = 4245 \pm 20$ ppm, which indicates that the chemical shift of a XeF_2 molecule oriented perpendicular to the applied magnetic field, $\mathbf{B}_0$, gives rise to an NMR signal that is 4245 ppm less shielded than that of a molecule oriented parallel to $\mathbf{B}_0$. The observed xenon shielding anisotropy for XeF_2 is the largest measured for xenon[33] and represents the first direct measurement of Ω(Xe) for a xenon compound. The span of the shielding tensor for XeF_2 covers the entire known chemical shift range for Xe(II) compounds and approximately 70% of the total known xenon chemical shift range (~6200 ppm), as illustrated in Figure 3. The isotropic chemical shift range for Xe(II) compounds in various solvents is approximately 3400 ppm, ranging from −574 ppm for XeF^+ in SbF_5 at 25 °C to −3967.5 ppm for $C_6H_5Xe^+$ in HF at −10 °C.[35]

A striking feature of the ^{129}Xe NMR spectrum (Figure 3c) is the position of the parallel component of the chemical shift

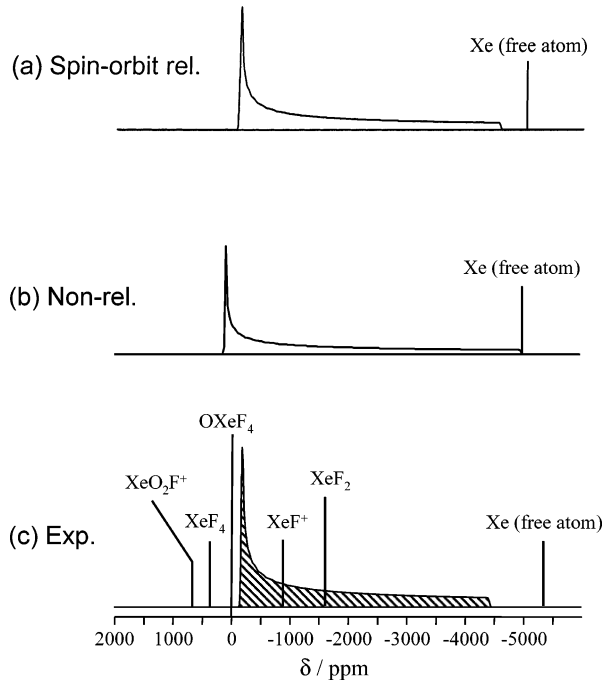

Figure 3. (a) Spin−orbit relativistic and (b) nonrelativistic ZORA DFT calculations of Ω(Xe) in XeF_2, assuming $\delta(^{129}Xe)_{iso} = -1603$ ppm. The isotropic ^{129}Xe chemical shift of the free Xe atom is shown with respect to $\delta(XeF_2)_{||}$, calculated using $\sigma(Xe(free\ atom))_{||} - \sigma(XeF_2)_{||}$ from Table 3. (c) Experimentally determined Ω(Xe) in XeF_2 and isotropic chemical shifts of selected xenon compounds plotted on the known xenon chemical shift scale.[79]

tensor, $\delta_{||} = -4433$ ppm, which differs from δ(Xe(free atom)) by ~1000 ppm! This observation is not in accord with nonrelativistic theory,[40,45] which predicts that $\sigma_{||} = \sigma_{||}^{dia} \simeq \sigma$(free atom) for any linear molecule, suggesting that relativistic effects play a significant role in determining nuclear magnetic shielding tensors for xenon. Our spin−orbit relativistic calculations are in agreement with experiment and indicate that the xenon free atom is ~430 ppm more shielded than $\sigma_{||}$ for XeF_2 (Figure 3a), whereas results from nonrelativistic calculations indicate that $\sigma_{||} \simeq \sigma$(free atom), as expected (Figure 3b). Hence, for relatively heavy nuclei such as xenon, it is clear that Ramsey's nonrelativistic theory[40] is not strictly applicable. Also, the spin−orbit relativistic results for Ω(Xe), 4469 ppm, are in excellent agreement with our experimental value, 4245 ± 50 ppm, with a relative difference, $[\Omega(Xe)_{exp} - \Omega(Xe)_{calc}]/\Omega(Xe)_{exp}$, of less than 10%, whereas the nonrelativistic value, 5067 ppm, is ~800 ppm greater than the experimental value. The dependence of σ_{iso}(Xe) on r(Xe,F) is small (see Table 8 of ref 80) at the relativistic level, $\partial\sigma(Xe)_{iso}/\partial r \simeq -403$ ppm Å^{-1}, but more pronounced at the nonrelativistic level, $\partial\sigma(Xe)_{iso}/\partial r \simeq -1016$ ppm Å^{-1}. Upon inspection of $\sigma_{||}$ for XeF_2 and KrF_2 at various bond lengths near r_e (not shown), considerable changes in $\sigma_{||}$ are observed for the relativistic calculations; however, calculations carried out at the nonrelativistic level as a function of bond length indicate that $\sigma_{||}$ remains constant for both XeF_2 and KrF_2, in accord with Ramsey's theory.[40,44] These results further stress the importance of relativistic effects in the xenon magnetic shielding of XeF_2 (Figure 3) and XeF_4 (Table 1). In particular, for XeF_4, inclusion of spin−orbit relativistic effects results in a dramatic change in Ω(Xe) from −204 to +1694 ppm. Comparison of results from σ(Xe) and σ(Kr) for XeF_2 and KrF_2 indicates that a significant decrease in the isotropic shielding and span is observed for Kr compared to Xe, as expected from the decrease in atomic number.[81] For σ(Kr) in KrF_2, inclusion of relativistic effects is less important.

TABLE 1: Calculated Magnetic Shielding Parameters for the Xenon Atom and Isolated XeF_2, XeF_4, and KrF_2 Molecules[a]

		$\sigma_{||}$/ppm	$\sigma_{\perp}$/ppm	σ_{iso}/ppm	Ω/ppm
		Spin−Orbit Relativistic DFT			
Xe (free atom)		6409.4	6409.4	6409.4	0
XeF_2	Xe	5976.6	1521.8	3006.7	4469.0
	F	523.8	246.6	339.0	277.2
XeF_4	Xe	1534.6	−159.7	405.0	1694.3
	F[b]	313.4	−48.0	177.9	361.4
KrF_2	Kr	3303.7	1312.2	1976.0	1991.6
	F	510.7	−161.2	62.8	671.9
		Nonrelativistic DFT			
Xe (free atom)		5646.7	5646.7	5646.7	0
XeF_2	Xe	5653.2	586.5	2275.4	5066.7
	F	496.8	297.2	363.7	199.6
XeF_4	Xe	−41.6	162.0	94.1	−203.5
	F[c]	271.3	−22.8	172.0	294.1
KrF_2	Kr	3255.8	1040.3	1778.8	2215.5
	F	492.8	−132.9	75.7	625.7

[a] Equilibrium geometries for XeF_2 from a Raman study and those for XeF_4 and KrF_2 from high-resolution infrared studies: r_e(Xe,F) in XeF_2 is 1.9791 Å, r_e(Xe,F) in XeF_4 is 1.928970 Å, and r_e(Kr,F) in KrF_2 is 1.87693 Å; refs 20, 74, and 75, respectively. [b] For XeF_4, σ(F) is nonaxially symmetric. The component along r(Xe,F) is $\sigma_{||} = \sigma_{33}$ and that parallel to the molecular C_4 symmetry axis is $\sigma_{\perp} = \sigma_{11}$, $\sigma_{11} = -48.0$ ppm, $\sigma_{22} = 268.3$ ppm, and $\sigma_{33} = 313.4$ ppm. [c] Assignment of $\sigma_{||}$ and $\sigma_{\perp}$ as in (b); $\sigma_{11} = -22.8$ ppm, $\sigma_{22} = 267.4$ ppm, and $\sigma_{33} = 271.3$ ppm.

TABLE 2: Xenon Magnetic Shielding and Indirect Nuclear ^{129}Xe,^{19}F Spin−Spin Coupling Values for XeF_2 from This Study and the Literature

method	Ω(Xe)/ppm	Ω(F)/ppm	$^1J(^{129}Xe,^{19}F)_{iso}$/Hz
solid-state NMR	4245 ± 20[a]	150 ± 20[d] 105[b]	−5560[d]
solution NMR[6]	2416 or 4722[d]	205[g]	5550 ± 20[e] 5644.2 ± 0.6[f]
semiempirical calcns	5125 or 7185[g]		
ZORA DFT	4469[d]	277[d]	−6038[h] −5958[i]

[a] This work. [b] Reference 22. [c] XeF_2 dissolved in acetonitrile-d_3. [d] Reference 24. [e] Reference 39. [f] Reference 23. [g] Reference 8. [h] Reference 15. [i] Reference 16.

It is now instructive to compare our Ω(Xe) results to those obtained in the literature; see Table 2. As previously mentioned, the work carried out by Jokisaari and co-workers[24] represents the first indirect measurement of Ω(Xe) from ^{129}Xe and ^{19}F T_1 studies of XeF_2 dissolved in acetonitrile-d_3. In favorable cases, interpretation of such data allows the determination of both Ω(Xe) and Ω(F) as well as the nuclear spin-rotation, SR, constants, $C_{\perp}(^{129}Xe)$ and $C_{\perp}(^{19}F)$. The analysis is complicated by the fact that one does not know the rotational correlation time, τ_2, or the angular momentum correlation time, τ_J. In the case of XeF_2 dissolved in acetonitrile-d_3, measurements of the spin−lattice relaxation rate, $R_1 = T_1^{-1}$, at variable temperatures and three different applied magnetic field strengths led to the conclusion that $\Omega(Xe)/\Omega(F) = 21.6 \pm 0.7$. Using the value of Ω(F), 105 ± 10 ppm, from early solid-state ^{19}F NMR measurements by Hindermann and Falconer,[22] and the ratio of the xenon and fluorine shielding anisotropies, 21.6, yields Ω(Xe) ≃ 2270 ppm. In an alternative approach, the authors recognized that the square root of the product of R_1^{CSA} and R_1^{SR} was independent of temperature and directly proportional to the applied magnetic field. In fact, one can show that

$$(R_1^{CSA}R_1^{SR})^{1/2} = \left(\frac{4}{135}\right)^{1/2}\left(\frac{m_e}{m_p}\right)\left(\frac{\gamma\hbar}{\mu_N}\right)(\gamma \mathbf{B}_0)\Omega^2 \qquad (3)$$

where m_e and m_p are the electron and proton rest masses, γ is the ^{129}Xe magnetogyric ratio, $\hbar$ is Planck's constant divided by 2π, μ_N is the nuclear magneton, and $\mathbf{B}_0$ is the applied magnetic field. An equivalent expression was used by Spiess and coworkers in analyzing ^{13}C T_1 relaxation data for liquid carbon disulfide.[82] This expression is valid under conditions where the Hubbard relationship[83] holds. Substitution of $(R_1^{CSA}R_1^{SR})^{1/2}$, determined from experiment, and the known constants into eq 3 led to Ω(Xe) = 4722 ppm, which is in fair agreement with our solid-state NMR value, 4245 ppm. In obtaining the above expression, we assume that the relationship between the nuclear spin-rotation tensor and magnetic shielding tensor is valid for xenon, a relatively heavy nucleus where relativistic effects are important.

Previous to the T_1 investigation of Jokisaari et al.,[24] the only data available for Ω(Xe) were the very early LCAO-MO calculations of Jameson and Gutowsky,[8] who, employing two different models, predicted that Ω(Xe) = 5125 or 7185 ppm. More recently, Jameson[9] made use of the approximation, $\Omega \approx -(3/2)[\sigma(XeF_2)_{iso} - \sigma(\text{free atom})]$, to estimate Ω(Xe), 5895 ppm; however, as previously mentioned, this result is based on a nonrelativistic model.

Listed in Table 3 are results for Ω(Xe), $C_\perp(^{129}Xe)$, and $C_\perp(^{19}F)$ in XeF_2, from the literature and this work. Our result for $C_\perp(^{129}Xe)$, 24.4 kHz, was calculated using our solid-state NMR value for Ω(Xe) and the relationship between Ω and $C_\perp$,[45] which is based on nonrelativistic theory. Although we have shown that relativistic effects are important for XeF_2, this exercise is carried out for the mere purpose of comparison with previous values. Jameson[9] followed the same approach, using Ω(Xe) = 5895 ppm, to calculate $C_\perp(^{129}Xe)$ and $C_\perp(^{19}F)$, −33.92 and −2.135 kHz, respectively; to a first approximation, the results are satisfactory. Jokisaari et al.[24] calculated the ^{129}Xe and ^{19}F spin-rotation constants according to the two aforementioned approaches. The first approach yielded values of 340 and 38.5 kHz for $C_\perp(^{129}Xe)$ and $C_\perp(^{19}F)$, respectively, whereas the second approach gave respective values of 174 and 19.7 kHz. We believe these values were mistakenly reported in kHz, but in fact are in rad s^{-1}. Dividing these values by 2π results in the values presented in Table 3. The value obtained for $C_\perp(^{129}Xe)$ calculated using the second approach, 27.7 kHz, is in reasonable agreement with those obtained here and those reported by Jameson.[9]

Expansions of a selected region of the ^{129}Xe NMR spectra of XeF_2 acquired *without* ^{19}F decoupling at two different spinning rates are shown in Figure 4. These spectra are characteristic of an AX_2-spin system influenced by both the direct, $R_{DD}(^{129}Xe,^{19}F)$, and indirect, $^1J(^{129}Xe,^{19}F)$, nuclear spin−spin coupling interactions. The *indirect* spin−spin coupling splits each spinning sideband into a triplet, corresponding to the three possible combinations of ^{19}F nuclear spin states, $m(^{19}F)$, of the two ^{19}F nuclei; i.e., $\Sigma m(^{19}F) = -1, 0, +1$. The magnitude of $^1J(^{129}Xe,^{19}F)_{iso}$, 5566 ± 50 Hz, is easily determined by measuring the splitting between the centerband and either satellite peak and confirmed by measuring this splitting at two different sample spinning rates. The ^{129}Xe,^{19}F *direct* dipolar interactions alter the relative intensities of the satellite peaks (Figure 4);[84]

$$R_{DD} = \gamma_{Xe}\gamma_F\left(\frac{\hbar}{2\pi}\right)\left(\frac{\mu_0}{4\pi}\right)\left\langle\frac{1}{r_{Xe,F}^{\ 3}}\right\rangle \qquad (4)$$

TABLE 3: Xenon Magnetic Shielding and Spin-Rotation Data for XeF_2

	Ω(Xe)/ppm	$\lvert C_\perp(^{129}Xe)\rvert$/kHz	$\lvert C_\perp(^{19}F)\rvert$/kHz
Jameson[a]	5895	33.92	2.135
Jokisaari et al.[b]	2416 and 4722	54.1 and 27.7	6.13 and 3.14
this work	4245	24.4	

[a] Reference 9. [b] Reference 24. Values of $C_\perp$ given in ref 24 have been divided by 2π.

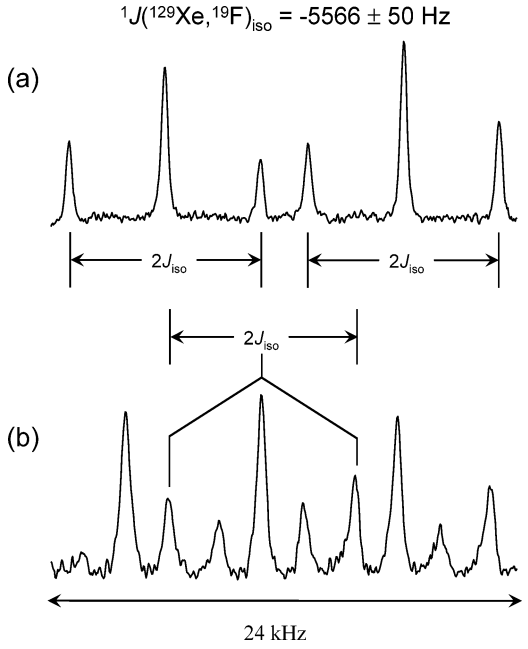

Figure 4. Expansions of ^{129}Xe NMR spectra of an MAS sample of XeF_2 acquired without ^{19}F decoupling at spinning frequencies of (a) 14.000 kHz and (b) 8.000 kHz.

where μ_0 is the vacuum permeability constant, $4\pi \times 10^{-7}$ kg m s^{-2} A^{-2}, and $\langle r_{XeF}^{-3}\rangle$ is the motionally averaged value of the inverse cube of the distance between xenon and fluorine. Experimentally, one measures the *effective* dipolar coupling, R_{eff}, which contains a contribution from the anisotropy of $\mathbf{J}_{iso}$, ΔJ:[84]

$$R_{eff} = R_{DD} - \frac{\Delta J}{3} \qquad (5)$$

For an AX_2 system, the relative signs of $^1J(^{129}Xe,^{19}F)_{iso}$ and R_{DD} may be determined, as outlined by Bai and Harris,[85] by analyzing the spinning sideband manifolds of the centerband and each of the satellite subspectra. If R_{eff} makes a significant contribution to the stationary line shapes, the effective spans of the satellite subspectra will differ: the subspectrum of one satellite will be stretched, whereas that of the other satellite will be squeezed with respect to the breadth of the central transition. In fact, one can show that the breadth of each subspectrum is given by[84]

$$\Delta\nu_{\pm m(^{19}F)} = (\nu_{||} - \nu_\perp) \pm 3\Sigma m(^{19}F)R_{eff} \qquad (6)$$

where $\Sigma m(^{19}F) = -1, 0, +1$. In the case of XeF_2, the centerband has a breadth of 235.9 kHz, the high-frequency spinning sideband manifold is stretched (breadth ≃ 248.8 kHz), and the low-frequency spinning sideband manifold is squeezed (breadth ≃ 219.7 kHz); making use of eq 6 gives $R_{eff} \simeq -4850 \pm 600$ Hz. Because only the relative signs of $^1J(^{129}Xe,^{19}F)_{iso}$ and $R_{DD}(^{129}Xe,^{19}F)$ can be determined, the absolute sign of either $^1J(^{129}Xe,^{19}F)_{iso}$ or $R_{DD}(^{129}Xe,^{19}F)$ must be known. For XeF_2, R_{DD} is negative as a consequence of the negative value of $\gamma(^{129}Xe)$.

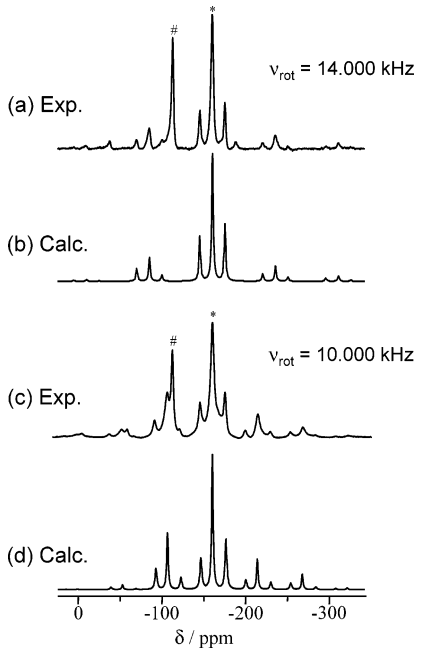

Figure 5. Experimental (a), (c) and calculated (b), (d) ^{19}F NMR spectra of an MAS sample of XeF_2. The isotropic ^{19}F chemical shifts for XeF_2 and the Teflon inserts of the rotor are indicated by * and #, respectively. The simulated ^{19}F NMR spectra do not include ^{19}F-^{19}F dipolar coupling, which contribute ~10% to the relative intensities of the spinning sidebands in the observed ^{19}F NMR spectra (see text).

This result, along with the fact that $\sigma_{||} > \sigma_{\perp}$, indicates that the relative signs of $^1J(^{129}Xe,^{19}F)_{iso}$ and $R_{DD}(^{129}Xe,^{19}F)$ are the same;[85] therefore, $^1J(^{129}Xe,^{19}F)_{iso}$ must be negative, -5560 ± 50 Hz. Analogous qualitative analysis of the ^{19}F NMR spectra obtained with MAS supports this conclusion, as well as results from recent ZORA DFT calculations on XeF_2.[15,16] The calculated values of $^1J(^{129}Xe,^{19}F)_{iso}$, -6030[15] and -5958 Hz,[16] are in very good agreement with our solid-state NMR value of $^1J(^{129}Xe,^{19}F)_{iso}$, -5560 ± 50 Hz, as well as the reported range of values from solution NMR in various solvents, ± 5579 to ± 5665 Hz.[23,39]

In some cases, ΔJ can be obtained from NMR spectra of isolated spin pairs.[86,87] Using the above result for R_{eff}, and making use of the known value of r(Xe,F) in XeF_2 to calculate R_{DD} (eq 4), one can determine ΔJ. Substitution of $R_{DD}(^{129}Xe,^{19}F) \simeq -4060$ Hz, calculated using r(Xe,F) = 1.9791 Å, and $R_{eff} \simeq -4850$ Hz into eq 5 gives $\Delta J = +2370$ Hz; the error in this value is estimated to be on the order of ± 1.8 kHz. Our experimental value for ΔJ, $+2380$ Hz, is of the same order of magnitude as that determined using ZORA DFT calculations, $\Delta J = 4048$ Hz.[15]

The ^{129}Xe NMR spectra indicate that $^1J(^{129}Xe,^{19}F)_{iso}$ is insensitive to temperature changes brought upon by sample heating at the spinning speeds employed in this study. Previous ^{129}Xe and ^{19}F NMR studies of XeF_2 in acetonitrile-d_3 also found that $^1J(^{129}Xe,^{19}F)_{iso}$ is insensitive to temperature changes over the range 240−320 K.[23]

4.2. ^{19}F NMR Spectroscopy. Shown in Figure 5 are experimental and calculated ^{19}F NMR spectra of XeF_2 acquired with MAS at two different spinning rates. Simulations of these spectra, using $^1J(^{129}Xe,^{19}F)_{iso} = -5560$ Hz, $R_{DD}(^{129}Xe,^{19}F) = 4064$ Hz, and assuming that the Xe, F dipolar vector and $\sigma_{||}$ are coincident, provides $\delta(^{19}F)_{iso} = -162 \pm 3$ ppm and $\Omega(F) = 160 \pm 20$ ppm. However, these simulations do not account for ^{19}F homonuclear dipolar coupling, which are known to contribute to the observed ^{19}F NMR line shape ($M_2^{homo} = 2.65$ G^2 or equivalently, 1.68×10^9 rad^2 s^{-2})[22] due to the proximity of neighboring fluorine atoms in the unit cell of XeF_2 (Figure 2). The significance of the ^{19}F−^{19}F dipolar interaction was subsequently investigated using an analytical method based on stochastic theory involving the memory function, which describes the time-averaged fluctuations of the local dipolar field.[88] The FID response function due to the dipolar interaction, obtained using the memory function approach, is given by[89]

$$G_D(t) = \exp\left\{M_2^{homo}\left[\frac{2}{3}f(\Gamma,\nu_{rot},t) + \frac{1}{3}(\Gamma,2\nu_{rot},t)\right]\right\} \qquad (7)$$

where

$$f(\Gamma,\nu_{rot},t) = \frac{1}{\Gamma^2 + \nu_{rot}^2} \times \left\{\frac{[(\Gamma^2 - \nu_{rot}^2)(1-\cos\nu_{rot}t) + 2\Gamma\nu_{rot}\sin\nu_{rot}t]\exp(-\Gamma t)}{\Gamma^2 + \nu_{rot}^2} - \Gamma t\right\}$$

and $\Gamma = 1/\tau_c$. Here, τ_c is the correlation time describing the stochastic process of the expectation values of the z-component of the spins due to the flip-flop operator and M_2 is the second moment. Simulations using $M_2^{homo} = 1.68 \times 10^9$ rad^2 s^{-2} suggest that ^{19}F−^{19}F dipolar coupling contributes ~10% to the line shape of the ^{19}F NMR spectrum of XeF_2 and that $\Omega(^{19}F) = 150 \pm 20$ ppm; this value for $\Omega(^{19}F)$ is within the error limits of that determined when ^{19}F−^{19}F dipolar coupling was neglected. Using our best solid-state NMR values for Ω(Xe), 4245 ppm, and Ω(F), 150 ppm, gives a ratio, Ω(Xe)/Ω(F), of 28.3, which is larger than that obtained by Jokisaari et al., 21.6,[24] suggesting that the xenon and fluorine shielding anisotropies may be different in solution and the solid state. The early solid-state ^{19}F NMR study by Hindermann and Falconer[22] determined Ω(F) to be 105 ± 10 ppm (vide supra); however, we believe the reported error to be underestimated. Jokisaari et al.[24] used the method based on eq 3 to determine Ω(F), 205 ppm, for XeF_2 in acetonitrile. There have been experimental reports of Ω(F) for XeF_4, ranging from 261 to 790 ppm,[90,91] and other main-group fluorides; solid-state ^{19}F NMR results indicate that for the series: SF_6, SeF_6, and TeF_6, Ω(F) is 310, 370, and 215 ppm, respectively.[92]

Experimental values of $\delta(^{19}F)_{iso}$ have previously been determined for XeF_2, XeF_4, and the XeF_6−tetramer in solution: -199.6, -15.7, $+118.3$ ppm.[35] The difference between $\delta(^{19}F)_{iso}$ for XeF_2 in solution and our solid-state NMR value, -162 ppm, is attributed to intermolecular effects, which are known to be predominantly deshielding.[93] Listed in Table 1 are ZORA DFT results for the shielding tensors in isolated XeF_2, XeF_4, and KrF_2 molecules. The *difference* in observed values of $\delta(F)_{iso}$ between XeF_2 and XeF_4, $\simeq 180$ ppm, agrees well with our calculated value, $\sigma(F)_{iso} \simeq 170$ ppm. In addition, our calculated values of Ω(F) for XeF_4 are within this range of observed values.[90,91] Calculations were not carried out on XeF_6 because it exists as a tetramer in solution[79] and in the solid state the structure is complicated by the presence of nondiscrete polymeric units.[94,95]

5. Conclusions

The xenon and fluorine magnetic shielding tensors in XeF_2 have been determined using solid-state ^{129}Xe and ^{19}F NMR spectroscopy and ZORA DFT calculations. The first direct experimental measurement of σ(Xe) for XeF_2 in the solid state is reported and the lingering question of the magnitude of the ^{129}Xe magnetic shielding anisotropy in this compound has been

resolved. The measured xenon anisotropy, $\Omega = 4245 \pm 20$ ppm, covers approximately 70% of the total known xenon chemical shift range. Analysis of ^{129}Xe NMR spectra allows determination of δ_{iso}, -1603 ± 3 ppm, and $^1J(^{129}Xe,^{19}F)_{iso}$, -5566 ± 50 Hz. Results from ^{19}F NMR spectra indicate that Ω(F), 150 ± 20 ppm, and that $^{19}F-^{19}F$ dipolar couplings contribute $\sim$10% to the observed ^{19}F NMR line shape. Spin−orbit relativistic ZORA DFT calculations of σ(Xe) are in excellent agreement with our solid-state NMR results, with a relative error less than 10%. Most important is that this study provides the first direct evidence that consideration of relativistic effects is important in interpreting xenon magnetic shielding tensors both experimentally and theoretically; however, questions remain. How far down the periodic table can one go before Ramsey's relativistic theory breaks down? Our spin−orbit calculations show that relativistic effects play a minor role for Kr, but a significant role for Xe. Also, what influence do relativistic effects have on nuclear spin-rotation constants and their relationship with nuclear magnetic shielding constants? Ongoing studies in our laboratory are being carried out to address this question.

Acknowledgment. We thank the members of the solid-state NMR group at the University of Alberta. In particular, we are grateful to Drs. Renée Siegel and Guy Bernard for valuable assistance and insightful discussions. R.E.W. is a Canada Research Chair in physical chemistry and thanks the Natural Sciences and Engineering Research Council (NSERC) of Canada for financial support. M.A.M.F. thanks the Alberta Ingenuity Fund, NSERC, and the University of Alberta for postgraduate scholarships.

References and Notes

(1) Khriachtchev, L.; Pettersson, M.; Runeberg, N.; Lundell, J.; Rasanen, M. *Nature* **2000**, *406*, 874−876.
(2) Pettersson, M.; Khriachtchev, L.; Lignell, A.; Rasanen, M.; Bihary, Z.; Gerber, R. B. *J. Chem. Phys.* **2002**, *116*, 2508−2515.
(3) Frenking, G.; Cremer, D. *Struct. Bonding* **1990**, *73*, 17−95.
(4) Khriachtchev, L.; Tanskanen, H.; Cohen, A.; Gerber, R. B.; Lundell, J.; Pettersson, M.; Kiljunen, H.; Rasanen, M. *J. Am. Chem. Soc.* **2003**, *125*, 6876−6877.
(5) Feldman, V. I., Sukhov, F. F.; Orlov, A. Y.; Tyulpina, I. V. *J. Am Chem. Soc.* **2003**, *125*, 4698−4699.
(6) Stein, L. *Nature* **1973**, *243*, 30−32.
(7) Holloway, J. H.; Hope, E. G. *Adv. Inorg. Chem.* **1999**, *46*, 51−100.
(8) Jameson, C. J.; Gutowsky, H. S. *J. Chem. Phys.* **1963**, *40*, 2285−2293.
(9) Jameson, C. J. In *Nuclear Magnetic Resonance: A Specialist Report*; Webb, G. A., Ed.; Royal Society of Chemistry: Cambridge, U.K., 1996; Vol. 25, Chapter 2, pp 38−82.
(10) Liao, M.-S.; Zhang, Q.-E. *J. Phys. Chem. A* **1998**, *102*, 10647−10654.
(11) Buth, C.; Santra, R.; Cederbaum, L. S. *J. Chem. Phys.* **2003**, *119*, 7763−7771.
(12) Styszyński, J.; Cao, X.; Malli, G. L. *J. Comput. Chem.* **1997**, *18*, 601−608.
(13) Bagus, P. S.; Liu, B.; Liskow, D. H.; Schaefer, H. F. *J. Am. Chem. Soc.* **1975**, *97*, 7216−7219.
(14) Malli, G. L. Styszyński, J. Dasilva, A. B. F. *Int. J. Quantum Chem.* **1995**, *55*, 213−225.
(15) Bryce, D. L.; Wasylishen, R. E. *Inorg. Chem.* **2002**, *41*, 3091−3101.
(16) Bagno, A.; Saielli, G. *Chem. Eur. J.* **2003**, *9*, 1486−1495.
(17) Smith, D. F. *J. Chem. Phys.* **1963**, *38*, 270−271. Tsao, P.; Cobb, C. C.; Claassen, H. H. *J. Chem. Phys.* **1971**, *54*, 5247−5253.
(18) Siegel, S.; Gerbert, E. *J. Am. Chem. Soc.* **1963**, *85*, 240.
(19) Levy, H. A.; Agron, P. A. *J. Am. Chem. Soc.* **1963**, *85*, 241−242.
(20) Brassington, N. J.; Edwards, H. G. M.; Long, D. A. *J. Chem. Soc., Faraday Trans. 2* **1978**, *74*, 1208−1213.
(21) Bürger, H. *J. Mol. Spectrosc.* **1993**, *157*, 536−539.
(22) Hindermann, D. K.; Falconer, W. E. *J. Chem. Phys.* **1969**, *50*, 1203−1205.
(23) Jokisaari, J. P.; Ingman, L. P.; Schrobilgen, G. J.; Sanders, J. C. P. *Magn. Reson. Chem.* **1994**, *32*, 242−247.
(24) Ingman, L. P.; Jokisaari, J.; Oikarinen, K.; Seydoux, R. *J. Magn. Reson.* **1994**, *111A*, 155−160.
(25) Cutler, J. N.; Bancroft, G. M.; Bozek, J. D.; Tan, K. H.; Schrobilgen, G. J. *J. Am. Chem. Soc.* **1991**, *113*, 9125−9131.
(26) Bürger, H.; Kuna, R.; Ma. S.; Breidung, J.; Thiel, W. *J. Chem. Phys.* **1994** *101*, 1−14.
(27) Lounila, J.; Oikarinen, K.; Ingman, P.; Jokisaari, J. *J. Magn. Reson.* **1996**, *118A*, 50−54.
(28) Mills, I.; Cvitaš, T.; Homann, K.; Kallay, N.; Kuchitsu, K. *Quantities, Units and Symbols in Physical Chemistry*, 2nd ed.; Blackwell Science: Oxford, U.K., 1993.
(29) Jameson, C. J, de Dios, A. C. *J. Chem. Phys.* **2002**, *116*, 3805−3821.
(30) Jameson, C. J., Sears, D. N., de Dios, A. C. *J. Chem. Phys.* **2003**, *118*, 2575−2580.
(31) Autschbach, J. Zurek, E. *J. Phys. Chem. A* **2003**, *107*, 4967−4972.
(32) Barrie, P. J., Klinowski, J. *Prog. Nucl. Magn. Reson. Spectrosc.* **1992**, *24*, 91−108.
(33) Ratcliffe, C. I. *Ann. Rep. Nucl. Magn. Reson. Spectrosc.* **1998**, *36*, 123−221.
(34) Jokisaari, J. *Prog. Nucl. Magn. Reson. Spectrosc.* **1994**, *26*, 1−26. And in: *Encyclopedia of Spectroscopy and Spectrometry*; Lindon, J. C., Tranter, G. E., Holmes, J. L., Eds.; Academic Press: San Diego, 1999; Vol. 3, pp 2435−2446.
(35) Gerken, M.; Schrobilgen, G. J. *Coord. Chem. Rev.* **2000**, *197*, 335−395.
(36) Raftery, D.; Chmelka, B. F. In *NMR, Basic Principles and Progress*; Diehl, P., Fluck, E., Günther, H., Kosfeld, R., Seelig, J., Eds.; Springer-Verlag: Berlin, 1994; Vol. 30, pp 112−158.
(37) Jameson, C. J. In: *Multinuclear NMR*; Mason, J., Ed.; Plenum Press: New York, 1987; Chapter 18, p 463.
(38) Schrobilgen, G. J. In *Encyclopedia of Nuclear Magnetic Resonance*; Grant, D. M., Harris, R. K., Eds.; John Wiley & Sons: Chichester, U.K., 1996; Vol. 5, p 3251.
(39) Seppelt, K.; Rupp, H. H. *Z. Anorg. Allg. Chem.* **1974**, *409*, 331.
(40) (a) Ramsey, N. F. *Molecular Beams*; Oxford University Press: London, 1956. (b) *Phys. Rev.* **1950**, *78*, 699−703.
(41) Pyykkö, P. *Theor. Chem. Acc.* **2000**, *103*, 214−216.
(42) Beeler, A. J.; Orendt, A. M.; Grant, D. M.; Cutts, P. W.; Michl, J.; Zilm, K. W.; Downing, J. W.; Facelli, J. C.; Schindler, M. S.; Kutzelnigg, W. *J. Am. Chem. Soc.* **1984**, *106*, 7672−7676.
(43) Dickson, R. M.; McKinnon, M. S.; Britten, J. F.; Wasylishen, R. E. *Can. J. Chem.* **1987**, *65*, 941−946.
(44) Jameson, C. J. In: *Encyclopedia of Nuclear Magnetic Resonance*; Grant, D. M., Harris, R. K., Eds.; John Wiley & Sons: Chichester, U.K., 1996; Vol. 2, pp 1273−1281.
(45) Flygare, W. H., Goodisman, J. *J. Chem. Phys.* **1968**, *49*, 3122−3125.
(46) Jameson, C. J. In *Multinuclear NMR*; Mason, J., Ed.; Plenum Press: New York, 1987; Chapter 3.
(47) Pyykkö, P. *Quantum Chemical Calculation of Magnetic Resonance Properties*; Kaupp, M., Bühl, M., Malkin, V., Eds. (in press).
(48) Vaara, J.; Malkina, O. L.; Stoll, H.; Malkin, V. G.; Kaupp, M. *J. Chem. Phys.* **2001**, *114*, 61−71.
(49) Manninen, P.; Lantto, P.; Vaara, J.; Ruud, K. *J. Chem. Phys.* **2003**, *119*, 2623−2637.
(50) Autschbach, J.; Ziegler, T. In *Encyclopedia of Nuclear Magnetic Resonance*, Grant, D. M., Harris, R. K., Eds.; Wiley: Chichester, U.K., 2002; Vol. 9, pp 306−323.
(51) Pyykkö, P.; Gorling, A.; Rosch, N. *Mol. Phys.* **1987**, *61*, 195−205.
(52) Pyykkö, P. *Chem. Phys.* **1983**, *74*, 1−7.
(53) Pyper, N. C. *Chem. Phys. Lett.* **1983**, *96*, 204−210, 211−217.
(54) Malli, G.; Froese, C. *Int. J. Quantum Chem., Suppl.* **1967**, *1*, 95−98.
(55) Kolb, D.; Johnson, W. R.; Shorer, P. *Phys. Rev. A* **1982**, *26*, 19−31.
(56) Kutzelnigg, W. *J. Comput. Chem.* **1999**, *20*, 1199−1219.
(57) Manninen, P.; Lantto, P.; Vaara, J.; Ruud, K. *J. Chem. Phys.*, **2003**, *119*, 2623−2637.
(58) Fukui, H.; Baba, T. *J. Chem. Phys.* **2002**, *117*, 7836−7844.
(59) Bennett, A. E.; Rienstra, C. M.; Auger, M.; Lakshmi, K. V.; Griffin, R. G. *J. Chem. Phys.* **1995**, *103*, 6951−6958.
(60) Eichele, K.; Wasylishen, R. E. *WSOLIDS NMR Simulation Package*, version 1.17.26, 2000.
(61) Bak, M.; Rasmussen, J. T.; Nielsen, N. C. *J. Magn. Reson.* **2000**, *147*, 296−330.
(62) Siegel, R.; Hirschinger, J.; Carlier, D.; Matar, S.; Ménétrier, M.; Delmas, C. *J. Phys. Chem. B* **2001**, *105*, 4166−4174.
(63) Harris, R. K.; Becker, E. D.; de Menezes, S. M. C.; Goodfellow, R.; Granger, P. *Pure Appl. Chem.* **2001**, *73*, 1795−1818.

(64) (a) Schreckenbach, G.; Ziegler, T. *J. Phys. Chem.* **1995**, *99*, 606−611. (b) Schreckenbach, G.; Ziegler, T. *Int. J. Quantum Chem.* **1997**, *61*, 899−918. (c) Wolff, S. K.; Ziegler, T. *J. Chem. Phys.* **1998**, *109*, 895−905.

(65) ADF 2000.02 and 2002.99, Theoretical Chemistry, Vrije Universiteit, Amsterdam, http://www.scm.com.

(66) (a) Baerends, E. J.; Ellis, D. E.; Ros, P. *Chem. Phys.* **1973**, *2*, 41−51. (b) Versluis, L.; Ziegler, T. *J. Chem. Phys.* **1988**, *88*, 322−328. (c) te Velde, G.; Baerends, E. J. *J. Comput. Phys.* **1992**, *99*, 84−98. (d) Fonseca Guerra, C.; Snijders, J. G.; te Velde, G.; Baerends, E. J. *Theor. Chem. Acc.* **1998**, *99*, 391−403.

(67) Vosko, S. H.; Wilk, L.; Nusair, M. *Can. J. Phys.* **1980**, *58*, 1200−1211.

(68) Becke, A. D. *Phys. Rev. A* **1988**, *38*, 3098−3100.

(69) Perdew, J. P. *Phys. Rev. B* **1986**, *33*, 8822−8824; **1986**, *34*, 7406−7406.

(70) Chang, C.; Pelissier, M.; Durand, P. *Phys. Scr.* **1986**, *34*, 394−404.

(71) van Lenthe, E.; Baerends, E. J.; Snijders, J. G. *J. Chem. Phys.* **1993**, *99*, 4597−4610.

(72) van Lenthe, E.; Baerends, E. J.; Snijders, J. G. *J. Chem. Phys.* **1994**, *101*, 9783−9792.

(73) van Lenthe, E.; van Leeuwen, R.; Baerends, E. J.; Snijders, J. G. *Int. J. Quantum Chem.* **1996**, *57*, 281−293.

(74) Bürger, H.; Ma, S.; Breidung, J.; Thiel, W. *J. Chem. Phys.* **1996**, *104*, 4945−4953.

(75) Bürger, H.; Kuna, R.; Ma, S.; Breidung, J.; Thiel, W. *J. Chem. Phys.* **1994**, *101*, 1−14.

(76) Vaara, J.; Pyykkö, P. *J. Chem. Phys.* **2003**, *118*, 2973−2976.

(77) (a) Jameson, C. J.; Jameson, K. A.; Burrell, P. M. *J. Chem. Phys.* **1980**, *73*, 6013−6021 (b) Jameson, C. J.; Jameson, K. A.; Honarbakhsh, J. *J. Chem. Phys.* **1984**, *81*, 5266−5267.

(78) Syvret, R. G.; Mitchell, K. M.; Sanders, J. C. P.; Schrobilgen, G. J. *Inorg. Chem.* **1992**, *31*, 3381−3385.

(79) Schrobilgen, G. J.; Holloway, J. H.; Granger, P.; Brevard, C. *Inorg. Chem.* **1978**, *17*, 980−987.

(80) Jameson, C. J. In *Encyclopedia of Nuclear Magnetic Resonance*; Grant, D. M., Harris, R. K., Eds.; John Wiley & Sons: Chichester, U.K., 1996; Vol. 4, p 2638.

(81) Jameson, C. J. In *Multinuclear NMR*; Mason, J., Ed.; Plenum Press: New York, 1987; Chapters 2 and 3.

(82) (a) Spiess, H. W.; Schweitzer, D.; Haeberlen, U.; Hausser, K. H. *J. Magn. Reson.* **1971**, *5*, 101. (b) Also discussed in: Spiess, H. W. In *NMR, Basic Principles and Progress*; Diehl, P., Fluck, E., Günther, H., Kosfeld, R., Eds.; Springer-Verlag: Berlin, 1978; Vol. 15, pp 55−214.

(83) Hubbard, P. S. *Phys. Rev.* **1963**, *131*, 1155.

(84) Wasylishen, R. E. In *Encyclopedia of Nuclear Magnetic Resonance*; Grant, D. M., Harris, R. K., Eds.; John Wiley & Sons: Chichester, U.K., 1996; Vol. 3, pp 1685−1695.

(85) (a) Bai, H.; Harris, R. K. *J. Magn. Reson.* **1992**, *96*, 24−30. (b) Cherryman, J. C.; Harris, R. K. *J. Magn. Reson.* **1997**, *128*, 21−29.

(86) VanderHart, D. L.; Gutowsky, H. S. *J. Chem. Phys.* **1964**, *49*, 261−271.

(87) Penner, G. H.; Power, W. P.; Wasylishen, R. E. *Can. J. Chem.* **1988**, *66*, 1821−1823.

(88) Mehring, M. *Principles of High-resolution NMR in Solids*; Springer: Berlin, 1983.

(89) (a) Kessemeier, H.; Norberg, R. E. *Phys. Rev.* **1967**, *155*, 321. (b) Reinheimer, P.; Hirschinger, J.; Gilard, P.; Goetz, N. *Magn. Reson. Chem.* **1997**, *35*, 757.

(90) Blinc, R.; Zupancic, I.; Maricic, S.; Veksli, Z. *J. Chem. Phys.* **1963**, *39*, 2109−2110.

(91) Hindermann, D. K., Falconer, W. E. *J. Chem. Phys.* **1970**, *52*, 6198−6202.

(92) Garg, S. K.; Ripmeester, J. A.; Davidson, D. W. *J. Magn. Reson.* **1980**, *39*, 317−323.

(93) Autschbach, J.; le Guennic, B. *J. Am. Chem. Soc.* **2003**, *125*, 13585−13593.

(94) Wells, A. F. *Structural Inorganic Chemistry*, 5th ed.; Clarendon Press: Oxford, U.K., 1984; p 377.

(95) Burbank, R. D. Jones, G. R. *J. Am. Chem. Soc.* **1974**, *96*, 43−48.